Bioorganic Chemistry 93 (2019) 103267

Contents lists available at ScienceDirect

Bioorganic Chemistry

journal homepage: www.elsevier.com/locate/bioorg

STAT3-inhibitory activity of sesquiterpenoids and diterpenoids from *Curcuma phaeocaulis*

Hyun-Jae Jang, Hyung-Jin Lim, Eun-Jae Park, Seung-Jae Lee, Soyoung Lee, Seung Woong Lee*, Mun-Chual Rho*

Immunoregulatory Materials Research Center, Korea Research Institute of Bioscience and Biotechnology, 181 Ipsin-gil, Jeongeup-si, Jeonbuk 56212, Republic of Korea

ARTICLE INFO

Keywords:
Curcuma phaeocaulis
IL-6
STAT3
Terpenes
Anti-inflammation

ABSTRACT

Three new sesquiterpenoids (compounds **4**, **5**, and **26**), along with 23 known sesquiterpenoids (compounds **1**–**3** and **6**–**25**) and two diterpenoids (compounds **27** and **28**), were obtained from *Curcuma phaeocaulis*, and their chemical structures were determined through nuclear magnetic resonance (NMR), circular dichroism (CD), and high-resolution electrospray ionization (HRESIMS) spectroscopic data, which were compared to the data from previous studies. All isolates were tested for inhibitory activity against interleukin (IL)-6-stimulated STAT3 expression using a luciferase reporter assay, and curzerenone (**21**) and 8-*epi*-galanolactone (**28**) displayed promising signal transducer and activator of transcription (STAT3)-inhibitory activities with IC_{50} values of 4.8 and 4.1 μM, respectively. In addition, these candidates significantly suppressed the mRNA expression levels of the proinflammatory genes IL-1β and C-reactive protein (CRP) via blockade of the IL-6-activated Janus kinase 2 (JAK2)/STAT3 and ERK-MAPK signaling pathways. These results suggest that curzerenone (**21**) and 8-*epi*-galanolactone (**28**) may be potential candidates for ameliorating severe inflammatory diseases.

1. Introduction

Interleukin-6 (IL-6), produced from monocytes, macrophages and T-cells during acute or chronic inflammation, is a primary upstream mediator of signal transducer and activator of transcription (STAT3) activation [1]. STAT3 regulates the transcription activity of various genes and contributes to cell proliferation, angiogenesis, survival, inflammation, neuroinflammation, and autoimmune diseases in the liver, adipose tissue, and blood [2–6]. IL-6 binds to its receptor complex, such as IL-6R and gp130, resulting in the dimerization and phosphorylation of gp130 and Janus kinase (JAK), and STAT3 is phosphorylated at tyrosine residues (Y^{705}) [5]. Phosphorylated STAT3 dimers are translocated into the nucleus to activate the transcription factors of various inflammatory genes [7]. Accordingly, the pathogenesis of many inflammatory diseases, including sepsis [8], liver injury [9], cancer cachexia [10], rheumatoid arthritis [11], and multiple myeloma [12], are associated with elevated IL-6 cytokine levels and elicited STAT3 activation via the IL-6/JAK/STAT3 pathway. Therefore, IL-6 signaling cascades may be useful molecular targets to prevent inflammatory disorders.

Curcuma phaeocaulis Val. (Zingiberaceae family) has been traditionally prescribed to improve blood circulation, arthralgia, dysmenorrhea, and liver diseases for centuries in the East Asian region, including China, Korea, and Japan [13,14]. Recent pharmacological studies have indicated that the rhizome of *C. phaeocaulis* has diverse biological activities, including anti-inflammatory, antioxidative, antitumor, hepatoprotective, and neuroprotective effects [14,15]. Previous studies on the phytochemical constituents of the genus Curcuma have revealed that diarylheptanoids and sesquiterpenoids are the main components of *Curcuma phaeocaulis* (*C. phaeocaulis*) [15–17]. To date, our research has also reported that the active anti-inflammatory components obtained from *C. phaeocaulis* are diarylheptanoid [18] and sesquiterpenoid [14] compounds.

In this paper, we examined whether the bioactive compounds obtained from *C. phaeocaulis* inhibit STAT3 expression and demonstrated whether the JAK2/STAT3 signaling pathway activated by IL-6 is negatively regulated by the compounds identified in our screening test.

2. Experiment

2.1. General experimental procedures

Proton (^1H) nuclear magnetic resonance (NMR) (600 MHz), carbon-13 (^{13}C) NMR (150 MHz), and two-dimensional (2D) NMR (correlation

* Corresponding authors.
E-mail addresses: lswdoc@kribb.re.kr (S.W. Lee), rho-m@kribb.re.kr (M.-C. Rho).

https://doi.org/10.1016/j.bioorg.2019.103267
Received 8 February 2019; Received in revised form 22 August 2019; Accepted 9 September 2019
Available online 10 September 2019
0045-2068/

spectroscopy (COSY), heteronuclear multiple-quantum correlation (HMQC), heteronuclear multiple bond correlation (HMBC), and nuclear overhauser effect spectroscopy (NOESY) spectra were measured on a JEOL JNM-ECA600 spectrometer with methanol-d_4 and chloroform-*d* solvents. High-resolution electrospray ionization (HRESIMS) data were obtained using a Bruker maXis 4G mass spectrometer (Bruker, Bremen, Germany). Optical rotations were determined on a Jasco P-2000 polarimeter (Jasco Corp., Tokyo, Japan), and ultraviolet (UV) spectra were recorded using a SpectraMax M_2^e spectrophotometer (Molecular Devices, Sunnyvale, CA, USA). Circular dichroism (CD) spectra were measured on a Jasco-J710 spectropolarimeter (Jasco Corp.), and infrared (IR) data were acquired using a Jasco-4600 FT-IR (Jasco Corp.). The *C. phaeocaulis* extract was fractionated using silica gel (Kieselgel 60, 230–400 mesh, Merck, Darmstadt, Germany) column chromatography (CC) and medium-pressure liquid chromatography (MPLC, CombiFlash RF, Teledyne Isco, Lincoln, NE, USA). The preparative high-performance liquid chromatography (HPLC) system consisted of a Shimadzu LC-6AD (Shimadzu Corp., Tokyo, Japan) pump equipped with an SPD-20A detector using Phenomenex Luna C_{18} (21.2 mm × 250 mm, 5 μm) columns.

2.2. Plant material

C. phaeocaulis rhizomes were acquired at an herbal store in Jeongeup, Korea. A voucher specimen (KRIBB-KR2014-700) of plant material was authenticated by one of the authors (M.-C. Rho) and has been deposited at the laboratory of Immunoregulatory Materials Research Center, Jeonbuk Branch of the Korea Research Institute of Bioscience and Biotechnology.

2.3. Extraction and isolation

Pulverized *C. phaeocaulis* rhizomes (4 kg) were subjected to extraction with EtOH (40 L × 3) for 7 days at room temperature. The ethanol extract was evaporated under reduced pressure, and the residue (283 g) was suspended in water (1.5 L) and successively partitioned with EtOAc (12 L) and BuOH (8 L). The EtOAc-soluble components (151 g) were concentrated *in vacuo* and chromatographed on silica gel (Kieselgel 60, 230–400 mesh, 150 g, Merck, Darmstadt, Germany), eluting with a gradient of *n*-hexane:EtOAc (1:0, 100:1, 50:1, 25:1, 10:1, 5:1, 2:1, 1:1, 0:1; v/v) to yield 38 fractions (CPE1–CPE38) based on the thin-layer chromatography (TLC) profile. CPE1 (12.3 g) was separated using MPLC eluted with H_2O:MeOH (C_{18} 130 g, 9:1 → 0:1, v/v) to give 18 subfractions (CPE1A–CPE1R). CPE1A (3.2 g) was purified by semipreparative HPLC (Phenomenex Luna C_{18}, 250 × 21.2 mm, 5 μm, 35% MeCN, 6 mL/min) to yield compounds **1** (7.4 mg), **7** (21.3 mg), and **21** (5.0 mg). CPE11 (1.7 g) was subjected to reverse-phase CC by using MPLC (C_{18} 130 g, H_2O:MeOH, 19:1 → 0:1, v/v) to obtain 23 subfractions (CPE11A − CPE11W). The subfractions CPE11B (34.1 mg), CPE11C (19.2 mg), CPE11K (91.5 mg), CPE11L (30.7 mg), CPE11R (49.8 mg), and CPE11V (32.4 mg) were purified by semipreparative HPLC (57%, 32%, and 72% MeOH, 6 mL/min) to yield compounds **14** (16.5 mg), **6** (8.0 mg), and **28** (12.1 mg). Compounds **22** (31.2 mg) and **3** (6.3 mg) were separated from CPE11O (105.5 mg) by semipreparative HPLC (55% MeOH, 6 mL/min). CPE14 (5.2 g) was chromatographed using MPLC (C_{18} 130 g, H_2O:MeOH, 7:3 → 0:1, v/v) to generate 17 subfractions (CPE14A − CPE14Q). CPE14D (815 mg) was further separated using MPLC (C_{18} 130 g, H_2O:MeOH, 100:1 → 0:1, v/v), and compounds **8** (15.3 mg), **12** (25.0 mg), **17** (3.2 mg), and **25** (6.4 mg) were isolated from the CPE14D3 (379 mg) subfraction by semipreparative HPLC (35% MeCN, 6 mL/min). CPE 14I (540 mg) subfraction was further purified to separate compound **15** (4.4 mg) using semipreparative HPLC (50% MeCN, 6 mL/min). CPE 17 (1.2 g) was subjected to MPLC with H_2O:MeOH (C_{18} 130 g, 100:1 → 0:1, v/v) to give 24 subfractions (CPE17A–CPE17X). Compound **26** (3.6 mg) was obtained from CPE17K (44.2 mg) using semipreparative HPLC (17% MeCN, 6 mL/min). CPE19 (2.3 g) was subjected to reversed-phase CC using MPLC (C_{18} 130 g, H_2O:MeOH, 4:1 → 0:1, v/v) to generate 16 subfractions (CPE19A–CPE17P). Semipreparative HPLC (20% MeCN, 6 mL/min) was used to isolate compound **24** (8.7 mg) from CPE19D (100.1 mg) and compounds **10** (9.8 mg) and **18** (17.1 mg) from the CPE19H (155.7 mg) subfractions. CPE25 (1.2 g) was separated by MPLC (C_{18} 130 g, H_2O:MeOH, 9:1 → 0:1, v/v) to give 20 subfractions (CPE25A–CPE25T). Compound **5** (5.3 mg) was purified from CPE25R (80.5 mg) using semipreparative HPLC (60% MeCN, 6 mL/min). CPE27 (7.1 g) was purified by MPLC (C_{18} 130 g, H_2O:MeOH, 9:1 → 0:1, v/v) to yield 17 subfractions (CPE27A–CPE27Q). Semipreparative HPLC (20% and 25% MeCN, 6 mL/min) was used to obtain compounds **19** (2.1 mg) and **11** (3.8 mg) from CPE27D (65.0 mg) and CPE27E (22.3 mg), respectively. Compounds **4** (4.2 mg) and **23** (23.0 mg) were isolated from CPE27P (67.2 mg) using semipreparative HPLC (30% MeCN, 6 mL/min). CPE28 (2.1 g) was separated by MPLC to give 15 subfractions (CPE28A–CPE28O). Compounds **20** (11.6 mg) and **13** (3.7 mg) were purified using semipreparative HPLC (21% and 30% MeCN, 6 mL/min) from CPE28D (36.4 mg) and CPE28E (68.2 mg), respectively. The BuOH-soluble components (46.2 g) were evaporated *in vacuo* and chromatographed on Diaion HP-20 resins, eluting with a mixture of H_2O and MeOH (9:1 → 0:1, v/v) to generate 10 subfractions (CPB1–CPB10). CPB5 (6.3 g) was separated by MPLC (C_{18} 130 g, H_2O:MeOH, 9:1 → 0:1, v/v) to obtain 12 subfractions (CPB5A–CPB5L). Compounds **16** (4.5 mg) and **27** (4.7 mg) were purified using semipreparative HPLC (35% MeCN, 6 mL/min) from CPB5E (508.0 mg). CPB9 (1.7 g) was chromatographed on Sephadex LH-20 resin to yield six subfractions (CPB9A–CPB9F), and compounds **9** (2.5 mg) and **2** (3.2 mg) were isolated using semipreparative HPLC (Phenomenex Luna C_{18}, 250 × 21.2 mm, 5 μm, 35% MeCN, 6 mL/min) from CPB9E (71.1 mg) Purity of compounds was confirmed by HPLC analysis (> 90%).

2.3.1. (−)-Phaeocaulin E (**4**)

Colorless syrup; $C_{15}H_{21}NO$; $[\alpha]_D^{25}$: −15.6 (*c* 0.1, MeOH); UV (MeOH) ν_{max} (logε) nm: 200 (2.13); IR (ATR): ν_{max} 3295, 2926, 2858, 1678, 1439, 1381, and 1074 cm^{-1}; CD (MeOH) λ_{max} (Δε) 231 (+0.14), 302 (−0.06), and 387 (+0.03) nm; ^1H and ^{13}C NMR spectra, see Table 1; HRESIMS: *m/z* 232.1696 $[M+H]^+$ (calcd for $C_{15}H_{22}NO$, 232.1696).

2.3.2. (+)-Phaeocaulin F (**5**)

Colorless syrup; $C_{16}H_{23}NO_2$; $[\alpha]_D^{25}$: +6.2 (*c* 0.1, MeOH); UV (MeOH) λ_{max} (logε) nm: 201 (2.16) and 258 (1.40); IR (ATR): ν_{max} 3303, 2927, 2862, 1697, 1449, 1382, and 1087 cm^{-1}; CD (MeOH) λ_{max} (Δε) 228 (−0.04), 278 (+0.08), 298 (−0.10), and 351 (−0.04) nm; ^1H and ^{13}C NMR spectra, see Table 1; HRESIMS: *m/z* 262.1802 $[M+H]^+$ (calcd for $C_{16}H_{24}NO_2$, 262.1802).

2.3.3. 12-Dehydroxy-chloraniolide a (**26**)

Yellow syrup; $C_{15}H_{22}O_3$; $[\alpha]_D^{25}$: +9.2 (*c* 0.1, MeOH); UV (MeOH) λ_{max} (logε) nm: 213 (2.05) and 261 (0.66); IR (ATR): ν_{max} 3452, 2918, 2856, 1742, 1462, 1384, 1231, 1088, and 883 cm^{-1}; ^1H and ^{13}C NMR spectra, see Table 1; HRESIMS: *m/z* 273.1461 $[M+Na]^+$ (calcd for $C_{15}H_{22}NaO_3$, 273.1461).

2.4. Cell culture and luciferase assay

Human hepatoma Hep3B and myeloma U266 cells were purchased from the American Type Culture Collection (ATCC No. HB-8064 and TIB-196TM, respectively, Rockville, MD, USA) and were cultured in Dulbecco's modified Eagle's medium (DMEM) and Roswell Park Memorial Institute (RPMI)-1640 medium supplemented with 10% fetal bovine serum (FBS, Gibco, Grand Island, NY, USA) and 100 U/mL penicillin-streptomycin (Gibco) at 37 °C in a 5% CO_2 incubator. Recombinant human IL-6 was obtained from R&D Systems (Minneapolis, MN, USA). All other reagents were obtained from Sigma-Aldrich Ltd. (St Louis, MO, USA).

Table 1
^{1}H (600 MHz) and ^{13}C NMR (150 MHz) data of compounds **4**, **5**, and **26**.[c]

Position	**4**[a]		**5**[a]		**26**[b]	
	δ_H (*J* in Hz)	δ_C	δ_H (*J* in Hz)	δ_C	δ_H (*J* in Hz)	δ_C
1	4.84, dd (11.4, 4.8)	130.8	4.78, dd (12.0, 4.2)	132.2	3.12, dt (10.2, 6.0)	48.7
2	2.26, m 2.06, br d (11.4)	26.9	2.31, qd (12.6, 4.2) 2.05, br d (12.6)	26.8	1.77, m[c]	24.9
3	2.22, m 1.88, td (12.6, 1.8)	39.6	2.23, m 1.94, td (11.4, 4.8)	39.6	1.83, m 1.76, m	38.2
4	–	133.0	–	134.6	–	82.6
5	4.38, d (11.4)	126.9	4.35, d (10.2)	126.3	2.52, dt (8.4, 6.0)	50.0
6	3.38, d (15.0) 2.96, dd (15.0, 11.4)	28.6	3.17, d (15.6) 2.83, dd (15.6, 10.2)	26.0	2.04, dd (15.0, 4.2) 1.98, dd (15.0, 8.4)	21.1
7	–	159.2	–	158.1	–	127.0
8	4.21, dd (12.0, 4.2)	61.2	–	96.9	–	156.4
9	2.87, br d (12.0) 1.94, t (12.0)	48.3	2.94, d (13.2) 2.22, d (13.2)	52.9	1.76, s	23.8
10	–	135.8	–	136.4	–	146.2
11	–	131.6	–	134.0	4.55, s	72.5
12	–	175.8	–	174.5	–	175.1
13	1.80, s	8.8	1.82, s	8.4	1.97, s	13.1
14	1.64, t (1.2)	17.1	1.62, t (1.2)	17.2	4.82, d (1.2) 4.72, br s	111.0
15	1.54, s	16.7	1.61, s	18.3	1.26, s	25.9
8-OCH_3	–	–	3.04, s	50.1	–	–

Data were measured in [a] methanol-d_4 and [b] chloroform-*d*.
[c] Overlapping.

2.5. Luciferase assay and cell viability

The stable hepatoma cells (Hep3B) transfected with pStat3-Luc used in a previous study [19] were seeded onto 96-well culture plates at 2×10^4 cells/well. After culturing for 24 h, the media were replaced with nonsupplemented DMEM for 12 h. Cells were preincubated with compounds for 2 h before stimulation with IL-6 (10 ng/mL) for 12 h. Luciferase activity was tested by using a Promega kit according to the manufacturer's instructions (Madison WI, USA). Cell viability was measured using the MTT method reported in a previous study [20].

2.6. Real-time polymerase chain reaction (PCR)

Real-time PCR was performed according to previously reported methods [18]. Briefly, total cellular RNA was extracted using a Pure Link RNA Mini Kit (Invitrogen, Carlsbad, CA, USA) following the manufacturer's protocol. The complementary DNA (cDNA) was synthesized using a Superscript III First-Strand Synthesis Super Mix for qRT-PCR (Invitrogen). Quantitative real-time PCR of C-reactive protein (CRP), IL-1β, ICAM-1 and SOCS3 was performed with a Taqman Gene Expression Assay kit (Applied Biosystems, Foster City, CA, USA). The gene expression was normalized using 18S rRNA. Quantitative real-time PCR was performed with TaqMan Gene Expression Master Mix on a Step One Plus Real-Time PCR System (Applied Biosystems) according to the manufacturer's instructions. Relative quantification of mRNA expression was performed using qPCRsoft software.

2.7. Western blot analysis

U266 cells were incubated with IL-6 (10 ng/mL) for 20 min in the presence or absence of compounds. Western blot analysis was performed to evaluate STAT3 and JAK2 protein expression in the U266 cell line, as described in previous studies [21]. All antibodies, phosphor-JAK2 (Tyr$^{1007/1008}$), phospho-STAT3 (Tyr^{705}), phospho-ERK (Tyr$^{202/204}$), JAK2, STAT3, and ERK were purchased from Cell Signaling Technology (Beverly, MA, USA). The phosphorylation status of STAT3 and JAK2 was examined using antiphospho-Stat3 (1:1000), anti-Stat3 (1:1000), antiphospho-Jak2 (1:1000), and anti-Jak2 (1:1000) antibodies (Cell Signaling) and then incubated with the appropriate horseradish peroxide-conjugated secondary antibody (1:2000). The optical densities of antibody-specific bands were quantified using ImageJ software.

2.8. Statistical analyses

The results are presented as the mean ± standard error of the mean (SEM), and all experiments were performed in triplicate. The statistical analyses were performed using Dunnett's test with Prism 5 software (GraphPad software, San Diego, CA, USA). $P < 0.05$ was considered statistically significant.

3. Results and discussion

The EtOH extract of *C. phaeocaulis* rhizomes suspended in H_2O was divided into EtOAc- (151 g) and BuOH-soluble (46 g) fractions, successively, which were subjected to silica gel CC, octadecyl silica (ODS) CC, MPLC and preparative HPLC to isolate the three previously undescribed sesquiterpenoids (**4**, **5**, and **26**) and the 25 known compounds, including germacrone (**1**) [22], 13-hydroxygermacron (**2**) [22], aeruginolactone (**3**) [23], (1*E*,4*Z*)-8-hydroxy-6-oxogermacra-1(10),4,7(11)-trieno-12,8-lactone (**6**) [24], furanodienone (**7**) [22], 1-hydroxy-isofuranodienone (**8**) [14], zederone (**9**) [25], curcolonol (**10**) [26], 9α-hydroxycurcolonol (**11**) [27], zedoaronfuran (**12**) [28], 3α-hydroxy-4-deoxy-5-dehydrocurcolonol (**13**) [28], myrrhterpenoid N (**14**) [29], 4α-hydroxy-8,12-epoxyeudesma-7,11-diene-1,6-dione (**15**) [24], 1β,4α-dihydroxy-5α,8β(*H*)-eudesm-7(11)*Z*-en-8,12-olide (**16**) [30], serralactone A (**17**) [31], neolitacumone A (**18**) [32], phaeusmane G (**19**) [15,33], 1β,4α-dihydroxyeudesm-7(11)-en-8-one (**20**) [34], curzerenone (**21**) [35], 8β-hydroxy-isogermafurenolide (**22**) [36], 8β(*H*)-elema-1,3,7(11)-trien-8,12-lactam (**23**) [37], phacadinane B (**24**) [38], phacadinane D (**25**) [38], coronarin I (**27**) [39], and 8-*epi*-galanolactone (**28**) [40] (Fig. 1). All isolates were evaluated for STAT3 inhibitory activity using Hep3B cells stably expressing pSTAT3-Luc established in a previous study.

Compound **4** was obtained as a colorless syrup with $[\alpha]_D^{25}$ −15.6 (MeOH, *c* 1.0). Its molecular formula, $C_{15}H_{22}NO$, was determined from the HRESIMS data (*m/z* 232.1696 $[M+H]^+$, calculated as 232.1696). The IR spectrum displayed the presence of an unsaturated lactam group

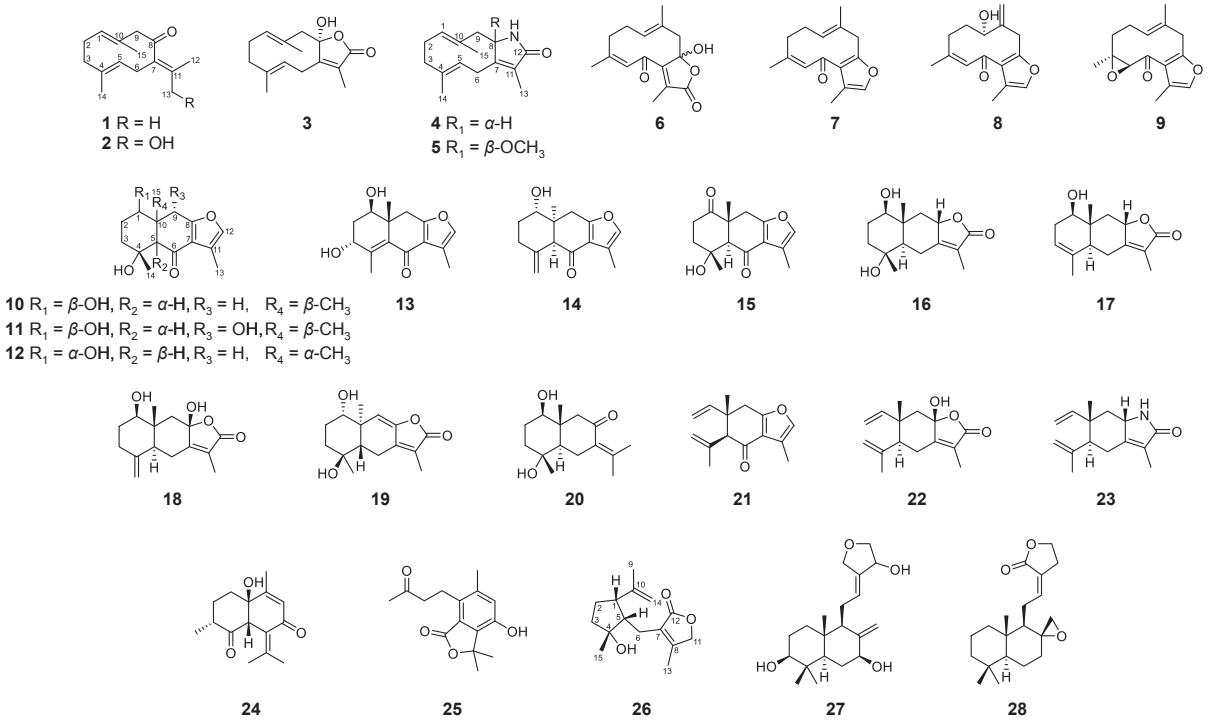

Fig. 1. Chemical structures of compounds **1–28**.

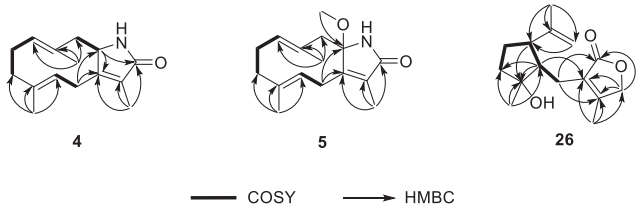

Fig. 2. Key COSY and HMBC correlations of compounds **4**, **5**, and **26**.

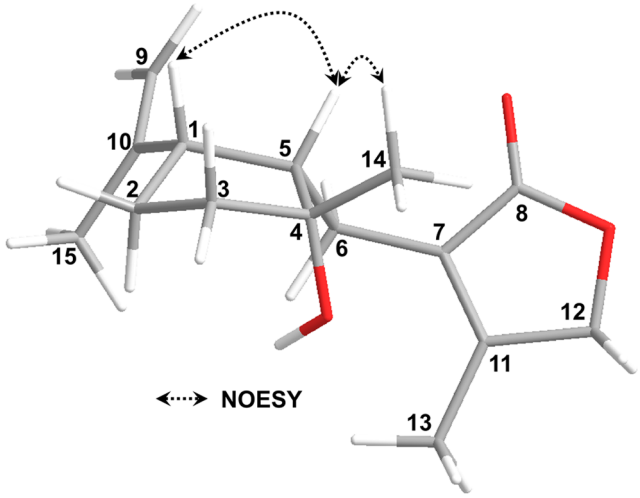

Fig. 3. Key NOESY correlations of compound **26**.

at 3295 and 1678 cm^{-1} [37,41]. The ^1H NMR spectrum of compound **4** revealed three olefinic methyl protons [δ_H 1.80 (s, H_3-13), 1.64 (t, J = 1.2 Hz, H_3-14), and 1.54 (s, H_3-15)], four methylene protons [δ_H 3.38 (d, J = 15.0 Hz, H-6a), 2.96 (dd, J = 15.0, 11.4 Hz, H-6b), 2.87 (br d, J = 12.0 Hz, H-9a), 2.26 (m, H-2a), 2.22 (m, H-3a), 2.06 (br d, J = 11.4 Hz, H-2b), 1.94 (t, J = 12.0 Hz, H-9b), and 1.88 (td, J = 12.6, 1.8 Hz, H-3b)], two olefinic protons [δ_H 4.84 (dd, J = 11.4, 4.8 Hz, H-1) and 4.38 (d, J = 11.4 Hz, H-5)], and one methine proton adjacent to the lactam moiety [δ_H 4.21 (dd, J = 12.0, 4.2 Hz, H-8)]. The ^{13}C and distortionless enhancement by polarization transfer (DEPT) NMR spectroscopic data displayed signals for 15 carbon resonances, including one carbonyl carbon [δ_C 175.8 (C-12)], six olefinic carbons [δ_C 159.2 (C-7), 135.8 (C-10), 133.0 (C-4), 131.6 (C-11), 130.8 (C-1), and 126.9 (C-5)], one methine carbon adjacent to the secondary amine group [δ_C 61.2 (C-8)], four methylene carbons [δ_C 48.3 (C-9), 39.6 (C-3), 28.6 (C-6), and 26.9 (C-2)], and three methyl carbons [δ_C 17.1 (C-14), 16.7 (C-15), and 8.8 (C-13)]. The COSY cross peaks between H-1/H_2-2/H_2-3, H-5/H_2-6, and H-8/H_2-9 and the HMBC cross peaks between H-2/C-4, H_3-15/C-3/C-4/C-5, H-6/C-7/C-8, H-8/C-12, H_3-13/C-7/C-11/C-12, and H_3-14/C-1/C-9/C-10 support the suggestion that the structure of compound **4** was similar to that of phaeocaulin B (Fig. 2), which is a germacrane-type skeleton, except for a carbonyl group at C-6. The configurations of two double bonds were deduced from the ^{13}C NMR and NOESY data. The vinylic methyl carbon signals (C-14 and C-15) showed at a value of less than 20 ppm [42], and no correlations were observed from H-1/H_3-15 and H-5/H_3-14, suggesting that the $\Delta^{1(10)}$ and $\Delta^{4(5)}$ double bonds were assigned as (*E*)-configurations. Furthermore, the optical rotation of compound **4** was recorded as − 15.6 (*c* 0.1, MeOH), and its CD spectrum [(Δε) 231 (+0.14), 302 (−0.06), and 387 (+0.03) nm] was similar to that of (−)-phaeocaulin B [41], which was designated as 8*R*. Therefore, the structure of compound **4** was elucidated as (1*E*,4*E*,8*R*)-germacra-1(10),4,7,(11)-trieno-12,8-lactam and named (−)-phaeocaulin E.

Compound **5** was isolated as a colorless syrup, and its molecular formula of $C_{16}H_{23}NO_2$ was deduced from the HRESIMS data (*m/z* 262.1802 $[M+H]^+$, calculated as 262.1802). The IR, ^1H, and ^{13}C NMR spectroscopic data (Table 1) were similar to those of compound **4**, except for the presence of an additional methoxy group (δ_H 3.04 and δ_C 50.1) and the downfield carbon resonance peak at C-8 (δ_C 96.9) in compound **5**. The location of the methoxy group was assigned to C-8 in compound **5** on the basis of the HMBC correlation from OCH_3-8 to C-8 (Fig. 2). However, the different optical activities of compounds **4** and **5** ($[\alpha]_D^{25}$: +6.2*c* 0.1 in MeOH) indicated that the configuration at the chiral center (C-8) of compounds **4** and **5** may be opposite. The

Table 2
Inhibitory effects of compounds **1–28** on IL-6-stimulated STAT3 expression.[a]

Compounds	IC_{50} (μM)	Compounds	IC_{50} (μM)	Compounds	IC_{50} (μM)
1	> 50	**11**	> 50	**21**	4.8 ± 1.3
2	41.3 ± 3.5	**12**	> 50	**22**	> 50
3	> 50	**13**	> 50	**23**	15.3 ± 1.3
4	35.3 ± 6.8	**14**	> 50	**24**	> 50
5	28.6 ± 2.7	**15**	20.3 ± 3.3	**25**	46.8 ± 3.7
6	> 50	**16**	> 50	**26**	> 50
7	> 50	**17**	> 50	**27**	> 50
8	27.4 ± 2.8	**18**	> 50	**28**	4.1 ± 0.5
9	13.4 ± 1.5	**19**	> 50		
10	> 50	**20**	> 50		

Data are shown as the IC_{50} values (mean ± SEM) of three independent experiments ($n = 3$).
[a] No cytotoxicity was observed at the IC_{50} concentration. Stattic, selective STAT3 inhibitor [44], was used as the positive control (IC_{50}: 0.16 ± 0.04).

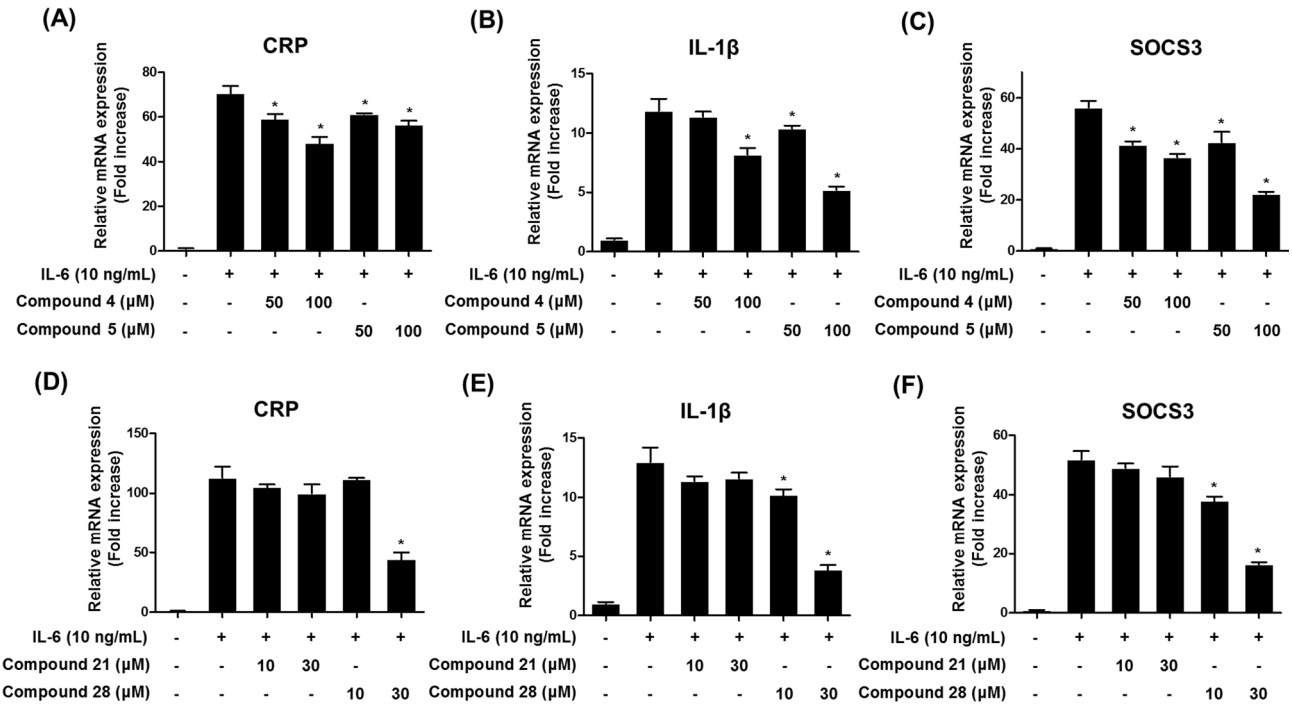

Fig. 4. Effect of compounds **4**, **5**, **21**, and **28** on the mRNA expression of CRP, IL-1β, and SOCS3 in IL-6-stimulated cells. Hep3B cells were preincubated with compounds (A, B, C) **4**, **5**, (D, E, F) **21**, and **28** for 1 h before treatment with IL-6 (10 ng/mL) for 5 h. Real-time PCR was used to analyze mRNA expression, and the data are expressed as the mean ± SEM of three independent experiments. *$P < 0.05$ compared to the IL-6-only group was considered statistically significant.

similarity of the CD spectrum between compound **5** [(Δε) 228 (−0.04), 278 (+0.08), and 351 (−0.04) nm] and the previously reported compound, (+)-phaeocaulin A, supported that the absolute configuration at C-8 in compound **5** was determined to be *S*. Thus, the structure of compound **5** was deduced as (1*E*,4*E*,8*S*)-8-methoxy-germacra-1(10),4,7,(11)-trieno-12,8-lactam and named (+)-phaeocaulin F.

Compound **26** was purified as a yellow syrup, and its molecular formula of $C_{15}H_{22}O_3$ was deduced from a sodium adduct ion in the HRESIMS data at *m/z* 273.1461 ($[M+Na]^+$, calculated as 273.1461). The IR spectrum showed absorption bands for hydroxy (3452 cm^{-1}) and α,β-unsaturated γ-lactone (1742 cm^{-1}) [16] groups. The ^1H and ^{13}C NMR spectra indicated resonances of tertiary methyl [δ_H 1.26 (s, H_3-15); δ_C 25.9 (C-15)], isopropenyl [δ_H 4.82 (d, $J = 1.2$ Hz, H-14a), 4.72 (br s, H-14b), and 1.76 (s, H_3-9); δ_C 111.0 (C-14), 146.2 (C-10), and 23.8 (C-9)], and α,β-unsaturated γ-lactone [δ_H 4.55 (s, H-11), and 1.97 (s, H_3-13); δ_C 127.0 (C-7), 175.1 (C-12), 156.4 (C-8), 72.5 (C-11), and 13.1 (C-13)] groups (Table 1). These NMR spectroscopic data were similar to those of chloraniolide A [43], and the HMBC correlations from H_2-12 to C-7/C-11/C-8 supported that the chemical structure was absent from the secondary alcohol on the lactone moiety in chloraniolide A (Fig. 2). The nuclear overhauser effect (NOE) correlations between H-1 and H-5 and between H-5 and H_3-14 suggest that configurations of H-1, H-5, and H_3-14 were β-oriented (Fig. 3). Accordingly, the structure of compound **26** was assigned and named 12-dehydroxy-chloraniolide A.

In our previous study, the ethanol extract of *C. phaeocaulis* and diarylheptanoids obtained from its ethyl acetate soluble fraction significantly suppressed IL-6/STAT3 expression in stable hepatoma cells (Hep3B) that were cotransfected with pSTAT3-Luc and pcDNA3.1/Hygro vector [18]. In addition, sesquiterpenoids (**1–26**) and diterpenoids (**27** and **28**) isolated from *C. phaeocaulis* were evaluated in the same manner to discover potent STAT3 inhibitors. Of the isolates, compounds **2**, **4**, **5**, **8**, **9**, **15**, **21**, **23**, **25**, and **28** showed inhibitory effects with IC_{50} values ranging from 4.1 to 46.8 μM (Table 2). Based on these bioassay results, we hypothesized that compound **21**, which is the main component of *C. phaeocaulis*, and compound **28** may be promising STAT3 inhibitors. CRP, which is a major acute phase protein in humans, and IL-1β are proinflammatory genes that are regulated by the IL-6 signaling pathway [45,46]. Accordingly, we investigated whether mRNA expression levels of the inflammation-related genes CRP and IL-

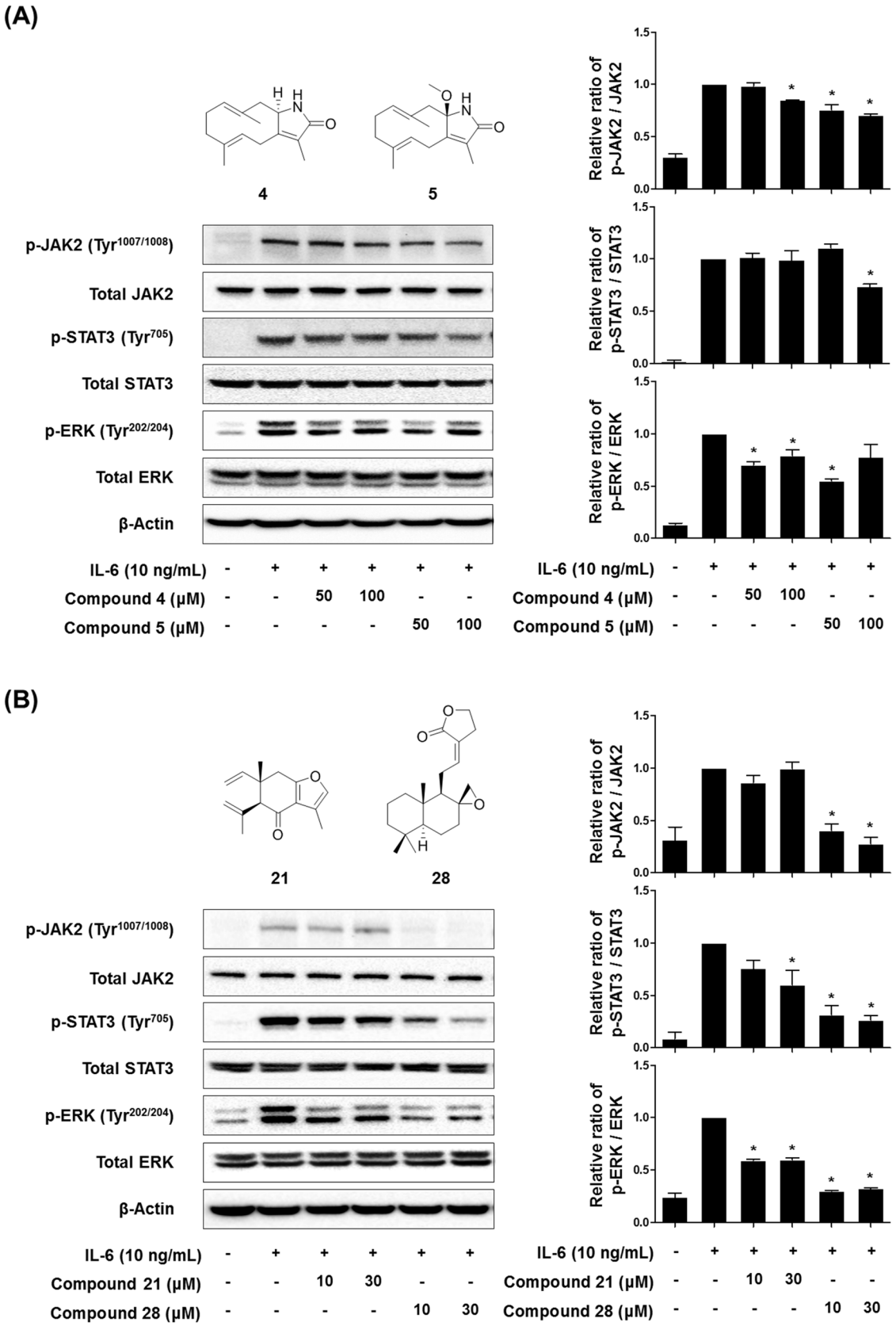

Fig. 5. Effects of compounds **4**, **5**, **21**, and **28** on the IL-6-induced phosphorylation of JAK2 STAT3 and ERK. U266 cells were pretreated with compounds (A) **4**, **5**, (B) **21**, and **28** for 1 h before stimulation with IL-6 (10 ng/mL). Whole cell lysates were subjected to Western blot analysis with specific antibodies against phospho-JAK2 ($Tyr^{1007/1008}$), phosphor-STAT3 (Tyr^{705}), phosphor-ERK ($Tyr^{202/204}$), JAK2, STAT3, ERK, and β-actin. The total nonphosphorylated proteins served as a loading control for the phosphorylated proteins. The band density was quantitated using ImageJ software, and the results are shown as the mean ± SEM. $^*P < 0.05$ versus the IL-6-only group was considered statistically significant.

1β were affected by the STAT3 inhibitor candidates using real-time PCR. As shown in Fig. 4, compounds **4**, **5**, **21**, and **28** dose-dependently and significantly inhibited the mRNA expression levels of the CRP and IL-1β genes through IL-6-activated cascades. Negative feedback regulation maintains homeostasis and is important for suppressing the development of immune or inflammatory diseases. Suppressors of cytokine signaling 3 (SOCS3) are negative feedback regulators that the IL-6-induced JAK/STAT3 signaling cascades blocked via interaction with JAK phosphotyrosine residues [47]. Thus, the inhibitory effects of SOCS3 on the IL-6-stimulated JAK/STAT3 pathway are involved in the blockade of the IL-6 signaling cascade. These results support the suggestion that compounds **4**, **5**, **21**, and **28** may suppress the IL-6-induced proinflammatory gene expression of CRP and IL-1β and the negative feedback inhibitor, SOCS3, via inhibition of JAK/STAT3 cascades. After JAK2 is phosphorylated in response to IL-6, activated STAT3 is translocated into the nucleus for the expression of proinflammatory genes [7]. IL-6 cytokines lead not only to JAK/STAT3 signaling but also to the induction of the ERK-MAPK pathway [48]. To further confirm whether the IL-6-stimulated JAK2/STAT3 and ERK-MAPK signaling pathways were affected by compounds **4**, **5**, **21**, and **28**, the phosphorylation of JAK2, STAT3, and ERK was detected by Western blot analysis. As shown in Fig. 5A, p-JAK2 and p-STAT3 protein levels were decreased by compounds **4** and **5**, and compound **5**, which has a methoxy group, exhibited a better inhibitory activity than compound **4** at 50 and 100 μM. As shown in Fig. 5B, compound **28** dose-dependently and significantly inhibited the phosphorylation of both JAK2 and STAT3; however, compound **21** significantly inhibited the phosphorylation only of STAT3 but not of JAK2. Thus, by activating STAT3, compound **21** may affect other cascades such as the epidermal growth factor receptor (EGFR) signaling pathway, which mediates both IL-6 secretion and STAT3 activation [49]. As shown in Fig. 5A and 5B, phosphorylation of ERK, which is a downstream target of EGFR cascades [50], was diminished by compounds **4**, **5**, **21**, and **28**. These results suggested that the STAT3 inhibitory effect of these compounds may be related to the IL-6-activated ERK-MAPK pathway.

In conclusion, three undescribed sesquiterpenoids (**4**, **5**, and **26**), together with 23 known sesquiterpenoids (**1–3** and **6–25**) and two diterpenoids (**27** and **28**), were identified in *C. phaeocaulis,* and their inhibitory effect was assessed using a luciferase assay to measure IL-6-stimulated STAT3 expression levels. Among these compounds, compound **28,** with the most potent inhibitory activity, significantly inhibited the mRNA expression of the proinflammatory genes IL-1β and CRP through the suppression of the JAK2/STAT3 and ERK-MAPK signaling cascades. Thus, further studies on the IL-6-related mechanism of 8-*epi*-galanolactone (**28**) may be helpful in developing therapeutic agents against inflammatory diseases.

Acknowledgments

This research was financially supported by the Agricultural Bio-industry Technology Development Program of the Ministry of Agriculture, Food, and Rural Affairs (314011-5) and a grant from the KRIBB Research Initiative Program (KGS9531911 and KGS9601911).

Appendix A. Supplementary material

Supplementary data to this article can be found online at https://doi.org/10.1016/j.bioorg.2019.103267.

References

[1] T. Kishimoto, Annu. Rev. Immunol. 23 (2005) 1–21.
[2] H. Yu, H. Lee, A. Herrmann, R. Buettner, R. Jove, Nat. Rev. Cancer 14 (2014) 736–746.
[3] M. Tsoli, M. Schweiger, A.S. Vanniasinghe, A. Painter, R. Zechner, S. Clarke, G. Robertson, PLoS One 9 (2014) e92966.
[4] H. Mori, R. Hanada, T. Hanada, D. Aki, R. Mashima, H. Nishinakamura, T. Torisu, K.R. Chien, H. Yasukawa, A. Yoshimura, Nat. Med. 10 (2004) 739–743.
[5] H. Wang, F. Lafdil, X. Kong, B. Gao, Int. J. Biol. Sci. 7 (2011) 536–550.
[6] J. Grisouard, T. Shimizu, A. Duek, L. Kubovcakova, H. Hao-Shen, S. Dirnhofer, R.C. Skoda, Blood 125 (2015) 2131–2140.
[7] H. Yu, D. Pardoll, R. Jove, Nat. Rev. Cancer 9 (2009) 798–809.
[8] L.A. Callahan, G.S. Supinski, Crit. Care Med. 37 (2009) S354–S367.
[9] B. Gao, Cell. Mol. Immunol. 2 (2005) 92–100.
[10] T.A. Zimmers, M.L. Fishel, A. Bonetto, Semin. Cell. Dev. Biol. 54 (2016) 28–41.
[11] N. Nishimoto, N. Miyasaka, K. Yamamoto, S. Kawai, T. Takeuchi, J. Azuma, Ann. Rheum. Dis. 68 (2009) 1580–1584.
[12] M. Fulciniti, T. Hideshima, C. Vermot-Desroches, S. Pozzi, P. Nanjappa, Z. Shen, N. Patel, E.S. Smith, W. Wang, R. Prabhala, Y.T. Tai, P. Tassone, K.C. Anderson, N.C. Munshi, Clin. Cancer Res. 15 (2009) 7144–7152.
[13] Y. Gan, S. Zheng, J. Zhao, C. Zhang, T. Gao, W. Liao, Q. Fu, C. Fu, J. Ethnopharmacol. 221 (221) (2018) 10–19.
[14] H.J. Jang, J.H. Kim, H.M. Oh, M.S. Kim, J.H. Jo, K. Jung, S. Lee, Y.H. Kim, W.S. Lee, S.W. Lee, M.C. Rho, Chem. Pharm. Bull. 64 (2016) 1062–1066.
[15] Y. Liu, J. Ma, Y. Wang, P.O. Donkor, Q. Li, S. Gao, Y. Hou, Y. Xu, J. Cui, L. Ding, F. Zhao, N. Kang, L. Chen, F. Qiu, Eur. J. Org. Chem. 25 (2015) 5540–5548.
[16] Y. Liu, J. Ma, Q. Zhao, C. Liao, L. Ding, L. Chen, F. Zhao, F. Qiu, J. Nat. Prod. 76 (2013) 1150–1156.
[17] Y.F. Hao, C.L. Lu, D.J. Li, L. Zhu, J.G. Jiang, J.H. Piao, Food Funct. 5 (2014) 1369–1373.
[18] H.J. Jang, E.J. Park, S.J. Lee, H.J. Lim, J.H. Jo, S.W. Lee, M.C. Rho, Planta Med. 85 (2019) 94–102.
[19] J.S. Chang, S.W. Lee, M.S. Kim, B.R. Yun, M.H. Park, S.G. Lee, S.J. Park, W.S. Lee, M.C. Rho, J. Pharmacol. Sci. 115 (2011) 84–88.
[20] H.J. Jang, S.J. Lee, S. Lee, K. Jung, S.W. Lee, M.C. Rho, Molecules 22 (2017) 1611.
[21] S.J. Lee, H.J. Jang, Y. Kim, H.M. Oh, S. Lee, K. Jung, Y.H. Kim, W.S. Lee, S.W. Lee, M.C. Rho, Process Biochem. 51 (2016) 2222–2229.
[22] J.H. Park, M.A. Mohamed, Y.J. Jung, S. Shrestha, T.H. Lee, C.H. Lee, D. Han, J. Kim, N.I. Baek, Arch. Pharm. Res. 38 (2015) 1752–1760.
[23] P.M. Giang, P.T. Son, K. Matsunami, H. Otsuka, Heterocycles 74 (2007) 977–981.
[24] B. Wu, S. He, X.D. Wu, Y.J. Pan, Chem. Biodivers. 5 (2008) 1298–1303.
[25] H. Shibuya, Y. Hamamoto, Y. Cai, I. Kitagawa, Chem. Pharm. Bull. 35 (1987) 924–927.
[26] W.J. Syu, C.C. Shen, M.J. Don, J.C. Ou, G.H. Lee, C.M. Sun, J. Nat. Prod. 61 (1998) 1531–1534.
[27] X. Yang, C. Wang, J. Yang, D. Wan, Q. Lin, G. Yang, Z. Mei, Y. Feng, Tetrahedron Lett. 55 (2014) 5632–5634.
[28] H. Matsuda, T. Morikawa, I. Toguchida, K. Ninomiya, M. Yoshikawa, Chem. Pharm. Bull. 49 (2001) 1558–1566.
[29] J. Xu, Y. Guo, P. Zhao, P. Guo, Y. Ma, C. Xie, D.Q. Jin, L. Gui, Fitoterapia 83 (2012) 801–805.
[30] S.P. Yang, C.R. Zhang, H.D. Chen, S.G. Liao, J.M. Yue, Chinese J. Chem. 25 (2007) 1892–1895.
[31] F. Teng, H.M. Zhong, C.X. Chen, H.Y. Liu, Helv. Chim. Acta 92 (2009) 1298–1303.
[32] F.R. Chang, T.J. Hsieh, T.L. Huang, C.Y. Chen, R.Y. Kuo, Y.C. Chang, H.F. Chiu, Y.C. Wu, J. Nat. Prod. 65 (2002) 255–258.
[33] H.J. Jang, S. Lee, S.J. Lee, H.J. Lim, K. Jung, Y.H. Kim, S.W. Lee, M.C. Rho, J. Nat. Prod. 80 (2017) 2666–2676.
[34] D.P. Piet, R. Schrijvers, M.C.R. Franssen, A. de Groot, Tetrahedron 51 (1995) 6303–6314.
[35] K.H. Shin, O.N. Kim, W.S. Woo, Arch. Pharm. Res. 12 (1989) 196–200.
[36] D. Friedrich, F. Bohlmann, Tetrahedron 77 (1988) 1369–1392.
[37] J.H. Ma, F. Zhao, Y. Wang, Y. Liu, S.Y. Gao, L.Q. Ding, L.X. Chen, F. Qiu, Org. Biomol. Chem. 13 (2015) 8349–8358.
[38] J. Ma, Y. Wang, Y. Liu, S. Gao, L. Ding, F. Zhao, L. Chen, F. Qiu, Fitoterapia 103 (2015) 90–96.
[39] P.V. Kiem, N.T. Thuy, T. Anh Hle, N.X. Nhiem, C.V. Minh, P.H. Yen, N.K. Ban, D.T. Hang, B.H. Tai, N.V. Tuyen, V.B. Mathema, Y.S. Koh, Y.H. Kim, Bioorg. Med. Chem. Lett. 21 (2011) 7460–7465.
[40] M. Jung, S. Lee, B. Yoon, Tetrahedron lett. 38 (1997) 2871–2874.
[41] G.Y. Xia, D.J. Sun, J.H. Ma, Y. Liu, F. Zhao, P. Owusu Donkor, L.Q. Ding, L.X. Chen, F. Qiu, Sci. Rep. 7 (2017) 43576.
[42] G.L. Lange, M. Lee, Magn. Reson. Chem. 24 (1986) 656–658.
[43] Y.J. Xu, C.P. Tang, M.J. Tan, C.Q. Ke, T. Wu, Y. Ye, Chem. Biodiversity 7 (2010) 151–157.
[44] D. Zhang, M. Sun, D. Samols, I. Kushner, J. Biol. Chem. 19 (1996) 9503–9509.
[45] M. Yamamoto, K. Yoshizaki, T. Kishimoto, H. Ito, J. Immunol. 164 (2000) 4878–4882.
[46] S.T. Ahmed, A. Mayer, J.D. Ji, L.B. Ivashkiv, J. Leukoc. Biol. 72 (2002) 154–162.
[47] P.C. Heinrich, I. Behrmann, S. Haan, H.M. Hermanns, G. Müller-Newen, F. Schaper, Biochem. J. 374 (2003) 1–20.
[48] Y. Wang, A.H. van Boxel-Dezaire, H. Cheon, J. Yang, G.R. Stark, Proc. Natl. Acad. Sci. USA 110 (2013) 16975–16980.
[49] V. Sriuranpong, J.I. Park, P. Amornphimoltham, V. Patel, B.D. Nelkin, J.S. Gutkind, Cancer Res. 63 (2003) 2948–2956.
[50] J. Schust, B. Sperl, A. Hollis, T.U. Mayer, T. Berg, Chem. Biol. 13 (2006) 1235–1242.